Technical Paper

Journal of the Society of Naval Architects of Korea
Vol. 35, No. 1, February 1998
大 韓 造 船 學 會 論 文 集
第 35 卷 第 1 號 1998年 2月

Numerical Investigations on Vortical Flows and Turbulence beneath the Free Surface around Bow

by

Uh-Cheul Jeong*, Yasuaki Doi** and Kazu-hiro Mori**

선수부 자유 표면 부근의 와 유동과 난류 특성에 관한 수치적 연구

정우철*, Yasuaki Doi**, Kasu-hiro Mori**

Abstract

Characteristics of turbulence beneath the free surface around a blunt bow are numerically investigated. Three dimensional Navier-Stokes and continuity equations are solved for the simulations. The Large Eddy Simulation(LES) with the external disturbance is performed to simulate the turbulent free surface flow called sub-breaking wave.

The result shows that the free surface fluctuates beyond a certain critical condition and the characteristics of the fluctuation are similar to the turbulent boundary layer flow around a solid body.

요 약

뭉툭한 스트럿에 의하여 생성되는 자유 표면의 난류 현상에 대한 기본 특성을 수치해석적 방법으로 연구하였다. 지배 방정식으로는 3차원 Navier-Stokes 방정식과 연속 방정식을 사용하였으며, 이들 지배 방정식은 유한 차분법으로 이산화 하였다. 물체앞 자유 표면에서의 난류 유동을 모사하기 위하여 임의의 작은 외부 교란을 도입하여 Large Eddy Simulation을 수행하였다.

물체앞 자유 표면은 어떠한 속도 이상에서 격렬하게 진동하는데 그 기본 특성은 물체 주위의 난류 흐름과 유사함을 수치 계산으로 보였다.

발 표 : 1997년도 대한조선학회 춘계연구발표회('97.4.26)
접수일자 : 1997년 8월 11일, 재접수일자 : 1998년 1월 19일
* 정회원, 삼성중공업(주) 조선/플랜트연구소
** 일본 히로시마대학 공학부

1. Introduction

Free surface flow around a surface piercing blunt bow is one of the most complicated phenomena in the field of ship hydrodynamics because of the various non-linear characteristics. Many researchers have studied the bow breaking wave with the hope of understanding how it affects the resistance of a ship.

Baba[1] proposed wave breaking resistance as a component of a ship resistance. He could provide quantitative evidences of a resistance component due to wave breaking around the bow by measuring head-loss using a wake survey method. Taneda and Amamoto[2] explained the bow breaking wave as a vortex motion. They called it "necklace vortex"(see Fig.1) to distinguish from a horseshoe vortex which was mainly generated by the boundary layer flow around the body mounted on the plate. Mori[3] explained that the necklace vortex was strongly related to the fluctuations of the free surface. He called this kind of fluctuations as "sub-breaking waves" in distinction from spilling or plunging breakers. However, the so-called bow breaking wave and the necklace vortex are not so simple and it may be very difficult to explain a single word "breaking". From these point of view, to make the phenomena clear, it is necessary to study the early stage where the breaking is apt to occur.

In the present paper, the characteristics of the sub-breaking wave generated by a free surface piercing vertical strut having NACA0012 wing section are numerically investigated. The investigations are made by solving the Navier-Stokes(RaNS) and continuity equations. The equations are discretized by a finite difference method(FDM) based on the MAC method. The fluctuated free surface flows are simulated by Large Eddy Simulation(LES) with the external disturbance. To simplify the problem, the surface tension is excluded in the present investigations.

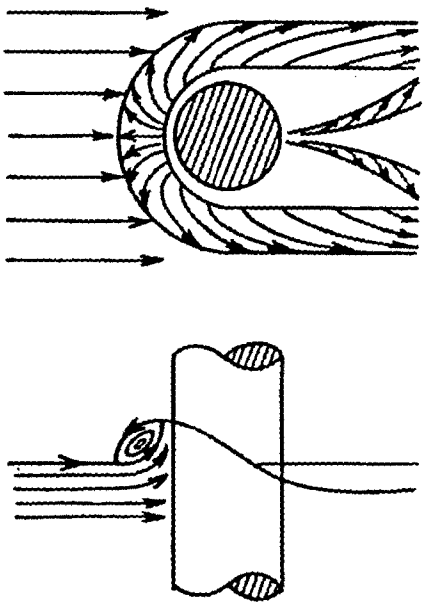

Fig.1 Schematic view of necklace vortex and vortical motion around circular cylinder, Taneda et al[2].

2. Observation of Bow Wave Patterns

An observation of bow wave patterns was performed for the vertical strut with NACA0012 section, which was the same as computed model, at the circulating water channel(CWC) of Hiroshima University. The length and draft of the models were 0.8m and 0.4m respectively. A plate painted white and black stripes was laid above the free surface and the pictures were taken from the bottom of the CWC. So the distortion of the images of stripes indicates the

free surface distortion. To remove a surface tension, a surfactant was used on the free surface[4].

As shown in Fig.2, there is no intensive distortion around bow at Fn=0.25 while strong distortion appears at Fn=0.30. The difference of velocity is about 0.14 m/s.

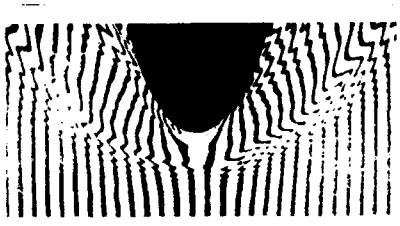

$(a) U = 0.70 m/s, Fn = 0.25, Rn = 3.9 \cdot 10^5$

$(b) U = 0.84 m/s, Fn = 0.30, Rn = 4.6 \cdot 10^5$

Fig.2 Free surface flows around bow.

Similar experiments were carried out by Mori[3]. He used two models which were circular cylinder and elliptic strut. He explained that the distortion of the free surface was strongly related to the fluctuations of the free surface. He called this kind of fluctuations as "sub-breaking waves" in distinction from spilling or plunging breakers. The basic characteristics of the sub-breaking wave will be discussed by numerical simulation later.

3. Numerical Algorithm and Boundary Conditions

3.1 Numerical algorithm and turbulence model

Three dimensional incompressible Reynolds averaged Navier-Stokes and continuity equations are employed for the present numerical study. The governing equations are written as follows;

$$\frac{\partial u_i}{\partial t} + u_j \frac{\partial u_i}{\partial x_j} = -\frac{\partial \Phi}{\partial x_i} + \frac{\partial}{\partial x_j}\left(\frac{1}{R_n}\frac{\partial u_i}{\partial x_j} - \overline{u_i' u_j'}\right) \quad (1)$$

$$\frac{\partial u_i}{\partial x_i} = 0 \quad (2)$$

$$-\overline{u_i' u_j'} = \nu_t\left(\frac{\partial u_i}{\partial x_j} + \frac{\partial u_j}{\partial x_i}\right) - \frac{2}{3} k\delta_{ij} \quad (3)$$

$$\Phi = p + \frac{z}{F_n^2} - P_{at} \quad (4)$$

where $u_i = (u, v, w)$and $x_i = (x, y, z)$ respectively in the Cartesian co-ordinate system as shown in Fig.3; x-axis in the uniform flow, y-axis in the lateral and z-axis in the vertical directions respectively. The origin is located at the leading edge of the strut on the undisturbed free surface. Fn, Rn, Φ, p, P_{at}, k and δ_{ij} are Froude number, Reynolds number, modified pressure, pressure, atmospheric pressure, turbulent energy and Kronecker delta respectively. All the variables are normalized by a uniform velocity, fluid density and the length of strut.

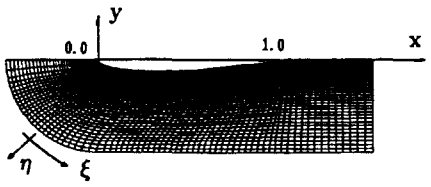

Fig.3 Coordinate systems and generated grid near body on horizontal plane.

The basic concept of the solution algorithm is based on the MAC method. A finite difference method is represented on a regular grid system. So, all the variables are defined on the grid nodes. The first order forward difference scheme is used for the time derivative terms. The convective terms are discretized by the third order upwind scheme. All the other spatial derivative terms are discretized by the second order centered difference scheme.

The Modified Baldwin-Lomax turbulence model(MBL) proposed by Degani and Schiff[5] is used to simulate the turbulent flow around the body and it is assumed that the turbulent flow starts at x=0.1.

One of the important characteristics of the sub-breaking waves is the intensive fluctuations of the free surface. In order to simulate the sub-breaking waves efficiently the Large Eddy Simulation(LES) with sub-grid-scale(SGS)[6] is locally performed around bow where the fluctuations can be intensive at a high Froude number as shown in Fig.2(b). Fig.4 shows the combination of the two different turbulent models(SGS and MBL). Between the two regions, an intermediate region(INT) is assumed to exist for matching the eddy viscosity. The eddy viscosity is smoothly changed in the streamwise direction through the INT where the eddy viscosity is calculated by mean value of SGS and MBL as follows;

$$(\nu_t)_I = \frac{1}{2}[(\nu_t)_S + (\nu_t)_M] \tag{5}$$

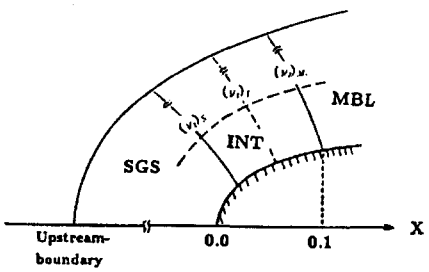

Fig.4 Combination of two different turbuence models(SGS and MBL).

As a trigger for the turbulence transition, the following artificial disturbance is introduced to the vertical velocity component on the free surface in SGS region for two successive time steps from T=4.0 and then removed.

$$w_d = \beta \cdot (0.2 \cdot u) \tag{6}$$

where β is a random constant ($-1.0 \le \beta \le 1.0$) and u is the calculated velocity component in the x-direction.

3.2 Boundary conditions

3.2.1 Free surface boundary conditions

The free surface location can be calculated to satisfy the kinematic condition which represents that the fluid particles of the free surface always remain on it. In the present study, the following Euler-type kinematic condition is used.

$$h_t + uh_x + vh_y - w = 0 \tag{7}$$

where $h(x, y, t)$ is the wave elevation and the subscripts represent partial differentiations with respect to the referred variables. The equation

is discretized by the first order upwind scheme for the time integration and the third order upwind scheme for other terms.

On the other hand, the velocity and pressure can be calculated by an equilibrium of stresses on the free surface as follows;

$$\sigma_{ij}n_j = \sigma^*_{ij}n_j \tag{8}$$

$$\sigma_{ij} = -p\delta_{ij} + \frac{1}{Rn}\left(\frac{\partial u_i}{\partial x_j} + \frac{\partial u_j}{\partial x_i}\right) - \overrightarrow{u_i u_j} \tag{9}$$

where σ_{ij} , σ^*_{ij} and n_j are fluid stress tensor, external stress tensor and unit outward normal vector to the free surface respectively in the Cartesian coordinate system. Assuming no shear stress and excluding the surface tension, the equation(8) can be rewritten as follows;

$$\sigma_{ij}n_j n_i = P_{at} \tag{10}$$

$$\sigma_{ij}n_j t_i = 0 \tag{11}$$

where t_i is the unit tangential vector to the free surface.

The above no shear stress condition can be expressed in 2-dimensional streamline curvilinear coordinate system as follow[7];

$$\omega = 2\kappa q_s \tag{12}$$

where, ω, κ and q_s are vorticity, free surface curvature and streamwise velocity on the free surface respectively. Equation(12) means that the free surface curvature can generate the vorticity if the streamwise velocity is not zero.

3.2.2 Other boundary conditions

On the body surface, no-slip condition is applied for the velocity and Neumann-type condition for the pressure. Because a strict treatment of the intersection region between the free surface and the solid body can not be expected due to the singularity, no-slip condition is used for the velocity while the wave elevation on the body is linearly extrapolated using neighboring wave elevations calculated by the kinematic free surface boundary condition. The pressure on the intersection is obtained by the dynamic free surface boundary condition directly.

A uniform velocity and zero wave elevation are applied on the inflow boundary and a zero-gradient extrapolation is used on all the outlet boundaries.

3.3 Grid generation

A numerical coordinate transformation is introduced into the body fitted coordinate system to simplify the computational domain and to facilitate the implementation of boundary conditions. C-H type grid is employed for the present computation. C-type grid is generated by using geometrical method[8] and the whole grid system is obtained by stacking them in the vertical direction algebraically. To fit the free surface boundary condition strictly, the moving grid system is introduced. The grid topology near body on a horizontal plane and the curvilinear coordinate system are shown in Fig.3. The ζ-axis of the body fitted coordinate system coincides with the z-axis. The grid lines are clustered near the body and the free surface to simulate properly the free surface and viscous interaction.

4. Results and Discussions

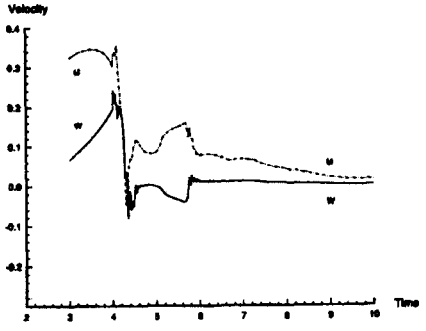

(a) $Fn = 0.25$

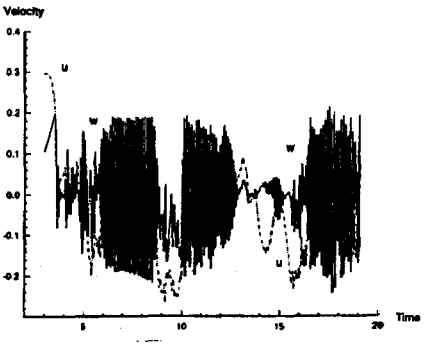

(b) $Fn = 0.30$

Fig.5 Computed time histories of velocity components.

Fig.5 shows the time histories of velocity components(u and) on the free surface at x =-0.025 and y=0.0, just in front of bow on the center plane, at Fn=0.25 and 0.30 and $Rn = 1.0 \cdot 10^6$. The disturbance, given by equation (6), is introduced on the free surface around T=4.0 for two time step. In the case of F_n=0.25 where no breaking is appeared as shown in Fig.2(a), the disturbance dies away after several time steps.

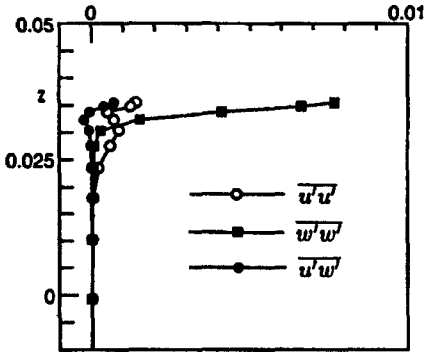

(a) Reynolds stresses

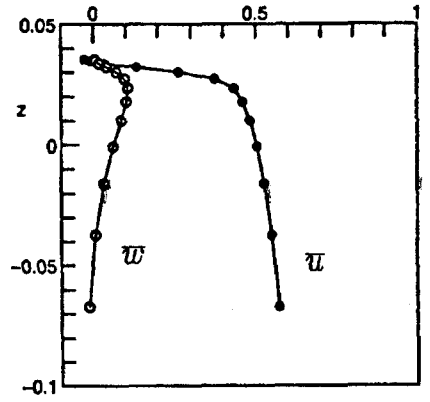

(b) Mean velocities

Fig.6 Computed Reynolds stress and mean velocity profiles, x=-0.025 and y=0.0, Fn=0.30.

On the other hand, in the case of Fn=0.30, the disturbance develops further and the final fluctuation seems irrelevant to the initially introduced disturbance. These results can explain that the free surface flow at Fn=0.25 is stable while it is unstable at Fn=0.30.

Fig.6 shows the computed Reynolds stress and mean velocity distributions at x=-0.025 and y=0.0 at Fn=0.30. Sharp defects of velocity

are observed close to the free surface both in $\overline{u}$ and $\overline{w}$ as measured in the experiments by Mori[3] and the turbulent intensity is also the same order as the experiments.

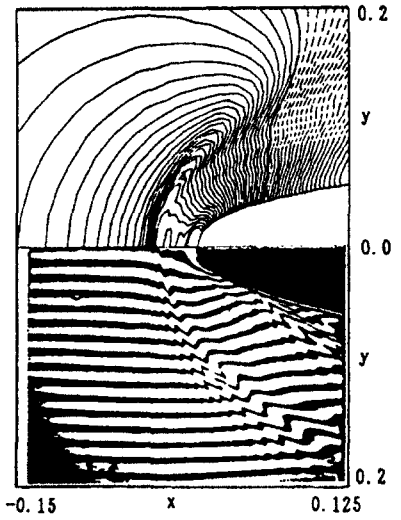

Fig.7 Comparison of computed and observed free surface flows, Fn=0.25.

Fig.7 shows a comparison of the computed and observed free surface flows at Fn=0.25. The Reynolds numbers for the computations and experiments are $1.0 \cdot 10^5$ and $3.8 \cdot 10^5$ respectively. It is noted that the flow fields around the bow are almost steady both in the experimental and computational results. The overall computed flow patterns agree well with the experimental results. The wave front lines are clearly shown in both results. The computed distance between the leading edge(x=0.0) and the wave front on the center plane is about 0.04L(x=-0.04)(L:length of the strut).

Fig.8 shows the computed vorticity(ω_y) and velocity distributions on the center plane in front of bow at Fn=0.25 and Rn= $1.0 \cdot 10^5$.

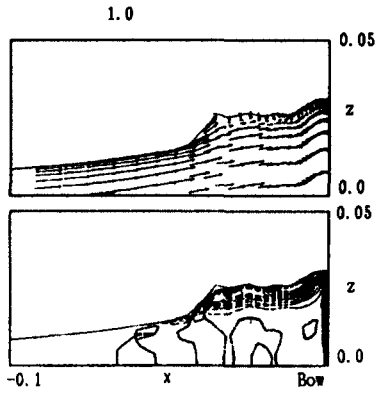

Fig.8 Computed velocity and vorticity (ω_y) distributions on center plane in front of bow, Fn=0.25.

The maximum vorticity is located just beneath the free surface. This is similar to the experimental result by Takekuma et al.[9] who reported that the vortical motions were located just below the free surface and the region did not extend widely so much and the depth was nearly as deep as the wave height.

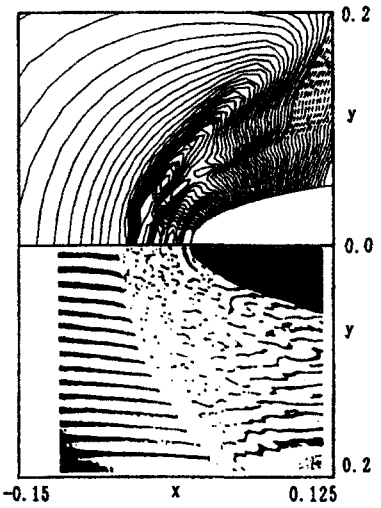

Fig.9 Comparison of computed and observed free surface flows, Fn=0.30.

Fig.9 shows the comparison of the computed and observed free surface flows around the bow at Fn=0.30. The Reynolds numbers of the computation and experiment are $1.0 \cdot 10^5$ and $4.6 \cdot 10^5$ respectively. The short-crested turbulent surface and the position of wave front line are well simulated. However, the computed wrinkles near bow seem smaller compared with the observed result. The reason may be not only that the grid system is still not fine enough to simulate the wrinkles but also that the surface tension is not considered in the computations.

Fig.10 shows the computed velocity and vorticity(ω_y) distributions on the center plane in front of bow. It must be noted that the flow around bow is still fluctuating. Although there are reverse flows in the bow wave field, they are not followed by overturning wave.

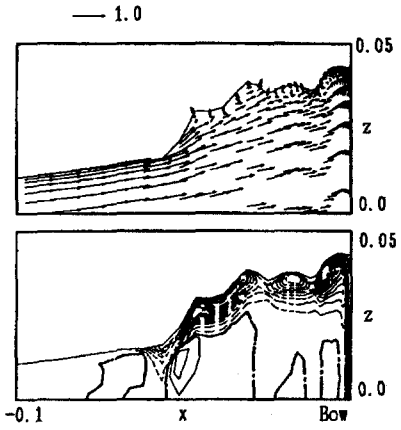

Fig.10 Computed velocity and vorticity (ω_y) distributions on center plane in front of bow, Fn=0.30.

The simulated results can explain that the free surface flow starts to fluctuate beyond a certain critical condition and the characteristics of the fluctuations are similar to the turbulent boundary layer flow around a solid body because the main features such as strong velocity defect(mean velocity) of main stream component and strong defect of Reynolds stress components close to the free surface is similar to those of the solid body in the turbulent flow.

5. Concluding Remarks

Basic characteristics of turbulent free surface flows called sub-breaking waves observed in experiments are numerically investigated. The free surface fluctuates beyond a certain critical condition and the characteristics of the fluctuations of the free surface are similar to the turbulent boundary layer flow around a solid body. Although the treatment of the surface tension has been left for future works, the newly developed scheme can disclose the precise mechanism of flow which are hard to clarify by experiments.

References

[1] Baba, E.:"A New Component of Viscous Resistance of Ship", Journal of the Society of Naval Architects of Japan, Vol.125, pp.23-34, 1969.

[2] Taneda, S. and Amamoto, H:"The Necklace Vortex of the Ship", Bulletin of Research Institute for Applied Mechanics, Kyushu Univ.,No.31, pp.17-28, 1969 (in Japanese).

[3] Mori, K:"Necklace Vortex and Bow Wave around Blunt Bodies",Proceedings of 15th Symposium on Naval Hydrodynamics, Hamburg, Germany, pp.303-317, 1984.

[4] Maruo, H. and Ikehata, H:"Some Discussions on the Free Surface Flow around the Bow, Proceedings of 16th Symposium on Naval Hydrodynamics, Berkeley, USA, pp.65-77,

1986.

[5] Degani, D. and Schiff, L. B.:"Computation of Turbulent Supersonic Flows around Pointed Bodies Having Crossflow Separation", Journal of Computational Physics, 66, pp.173-196, 1986.

[6] Deardorff, J. W.:"Numerical Study of Three Dimensional Turbulent Channel-Flow at Large Reynolds Numbers", Journal of Fluid Mechanics, 41, pp.453-480, 1970.

[7] Batchelor, G. K.:"An Introduction to Fluid Dynamics", Cambridge University Press, pp.364-366, 1970.

[8] Kodama, Y.:"Three Dimensional Grid Generation around a Ship Hull Using the Geometrical Method", Journal of the Society of Naval Architects of Japan, Vol.164, pp.1-8, 1988.

[9] Takekuma, K. and Eggers, K.:"Effect of Bow Shape on Free Surface Shear Flow",Proceedings of 15th Symposium on Naval Hydrodynamics, Hamburg, Germany, pp.387-405, 1984.